CHEMISTRY OF MATERIALS
Article

Chem. Mater. **2010,** *22,* 5957–5963 5957
DOI:10.1021/cm102204e

Template Synthesis of 3D High-Temperature Silicon-Oxycarbide and Silicon-Carbide Ceramic Photonic Crystals from Interference Lithographically Patterned Organosilicates

Yongan Xu,[†] Marta Guron,[‡] Xuelian Zhu,[†] Larry G. Sneddon,*[,‡] and Shu Yang*[,†]

[†]*Department of Materials Science and Engineering, University of Pennsylvania, 3231 Walnut Street, Philadelphia, Pennsylvania 19104, United States, and* [‡]*Department of Chemistry, University of Pennsylvania, 231 S 34th Street, Philadelphia, Pennsylvania 19104, United States*

Received August 3, 2010. Revised Manuscript Received September 26, 2010

The fabrication of 3D diamond-like silicon-oxycarbide and silicon-carbide high-temperature ceramic photonic crystals has been achieved by a strategy involving (1) the use of four-beam interference lithography (IL) to construct a patterned silsesquioxane (POSS) template and (2) infiltration of the polymeric allylhydridopolycarbosilane (AHPCS) silicon-carbide precursor into the patterned POSS template followed by high temperature ceramic conversion and HF etching. Energy-dispersive X-ray mapping analysis and Fourier transform infrared (FT-IR) studies suggested that the 3D ceramic photonic crystals formed at 1100 °C were SiC-like silicon oxycarbide. Additional thermal treatment at 1300 °C in vacuo resulted in the carbothermic reduction of the 3D silicon-oxycarbide to form 3D β-SiC with less than 10% shrinkage in the (111) plane and [111] direction, respectively. The reflectivities of the inverse 3D ceramic photonic crystals obtained at different stages were characterized by FT-IR in the [111] direction. Both the inverse 3D silicon-oxycarbide and silicon-carbide crystals showed bandgaps at 1.84 μm. These experimental values matched well with the calculated bandgaps, further supporting the robustness of such fabricated 3D ceramic photonic crystals.

Photonic crystals (PCs) that reflect incident light from any direction at a certain frequency range of light have the potential to provide revolutionary advances in next-generation microphotonic and opto-electronic devices. This potential has led to great interest in the development of both new materials and new fabrication techniques for the construction of one- (1D), two- (2D), and three-dimensional (3D) microstructures over large areas. While most PC applications are at room temperature with a few others up to 400 °C, PCs that can operate up to or higher than 1000 °C are essential for use in applications such as thermal barrier coatings (TBCs), selective emitters for thermophotovoltaics (TPV) and thermoelectrics.[1] For example, the TBC layer that is often applied to the combustor chamber of gas turbines to increase efficiency and reduce radiative heat transfer, must withstand temperatures in excess 1000 °C and intense infrared (IR) irradiation.[2,3] Such applications require a thermally and mechanically robust PC that is capable of withstanding prolonged exposure to high temperatures without any significant change in phase behavior, chemistry, or microstructure. Maintaining the integrity of the microsized lattice constants is undoubtedly the most critical issue of photonic structure design for high temperature applications.

Materials that have a high refractive index and are transparent in the near-IR and IR region are preferred, with the reflectivity in this region being determined by the particular photonic structure and material used. Both metals[4−7] and oxide ceramics have been previously employed as high temperature photonic materials. However, metallic photonic structures are readily degraded by corrosive environmental impurities, such as nitroxides, sulfur, chlorine, and water.[8] Metals also have higher thermal expansions than ceramics and are more prone to crack formation in the film. Oxide ceramics have high resistance to water corrosion at high temperature, but often have relatively low toughness.[9] Nonoxide ceramics have superior hardness, high melting points, low densities, and excellent thermal stability and silicon carbide (SiC), which has a high refractive

*Address correspondence to either author. E-mail: lsneddon@sas.upenn.edu (L. G. S.); shuyang@seas.upenn.edu (S. Y.).

(1) Shklover, V.; Mukherjee, L.; Witz, G.; Mishrikey, M.; Hafner, C. *J. Comput. Theor. Nanosci.* **2008**, *5*, 862.
(2) Clarke, D. R.; Levi, C. G. *Ann. Rev. Mater. Res.* **2003**, *33*, 383.
(3) Kelly, M. J.; Wolfe, D. E.; Singh, J.; Eldridge, J.; Zhu, D. M.; Miller, R. *Int. J. Appl. Ceram. Technol.* **2006**, *3*, 81.
(4) Seager, C. H.; Sinclair, M. B.; Fleming, J. G. *Appl. Phys. Lett.* **2005**, *86*, 244105.
(5) Lin, S. Y.; Moreno, J.; Fleming, J. G. *Appl. Phys. Lett.* **2003**, *83*, 380.
(6) Lin, S.-Y.; Fleming, J. G.; El-Kady, I. *Appl. Phys. Lett.* **2003**, *83*, 593.
(7) Nagpal, P.; Han, S. E.; Stein, A.; Norris, D. J. *Nano Lett.* **2008**, *8*, 3238.
(8) Visser, W. P. J.; Kluiters, S. C. A. *Modelling the Effects of Operating Conditions and Alternative Fuels on Gas Turbine Performance and Emissions*, NLR-TP-98629; National Aerospace Laboratory NLR: Amsterdam, 1998.
(9) Zawada, L. P.; Staehler, J.; Steel, S. *J. Am. Ceram. Soc.* **2003**, *86*, 1282.

Published on Web 10/14/2010

index ($n \sim 2.4-3.1$), has emerged as a promising material for many high temperature applications.[10−12]

TBCs composed of 1D SiC photonic crystals have previously been fabricated by layer-by-layer chemical vapor deposition (CVD) employing molecular ceramic precursors,[13−16] with the radiation reflectance of the resulting silicon-carbide TBC depending on the number of nanolayers. A high reflective index 3D PC could provide omnidirectional reflectance over all angles of incidence over a wide range of radiations, that is, a complete photonic bandgap (PBG), but the fabrication of such 3D ceramic photonic crystals for high temperature applications has not yet been achieved. We report here the successful fabrication of diamond-like silicon-oxycarbide and silicon-carbide high temperature PC ceramics via a strategy involving (1) the use of four-beam interference lithography (IL) to construct a patterned silsesquioxane (POSS) template and (2) infiltration of a polymeric silicon-carbide precursor into the patterned POSS template followed by high temperature ceramic conversion and HF etching to remove the template. The versatile ability of this IL/POSS templating method for generating structures with other symmetries should now allow the systematic fabrication of a wide variety of high temperature nonoxide ceramics with large and complete bandgaps.

Results and Discussion

Multibeam interference lithography is a powerful technique to fabricate 1D, 2D, and 3D photonic structures with (sub)micrometer periodicity over a large area with controlled defects. The symmetry of the resulting structures is controlled by the wave vectors and polarizations of the interfering beams. By subjecting the interfering beams to a photoresist using the same photochemistry developed in conventional lithography, a wide range of 3D photonic structures, including simple cubic (P), diamond (D), diamond-like, gyroid (G), quasi-crystals, and compound structures, can be designed and fabricated.[17,18]

The fabrication of a 3D PC with large and complete photonic bandgaps typically requires backfilling of high refractive index inorganic materials into a 3D microstructured silica or organic-polymer templates[18] and recently new materials chemistry and templating strategies have been developed to a range of such materials.[16,19−22] Since most polymer templates decompose above 500 °C,[23] they are not suitable for the fabrication of nonoxide ceramic PCs, where temperatures in excess of 1000 °C are required for most precursor ceramic conversions. More robust templates, with thermal and mechanical properties intermediate those of SiO_2 and organic polymers, can be formed from hybrid polyhedral oligomeric silsesquioxane (POSS) materials that are composed of cube-octameric Si-O Frameworks with eight organic corner groups. When functionalized with epoxy groups, the POSS molecules can be photo-cross-linked to form rigid structures. The nonreactive organic moieties make the POSS compatible with various polymer systems and enhance crack resistance.

We have previously reported the use of interference lithography to fabricate 3D photonic structures from epoxy-functionalized cyclohexyl polyhedral oligomeric silsesquioxane, including diamond-like structures by four-beam single exposure IL[24] and PCs with diamond symmetry via dual-beam quadruple exposure IL.[25] These POSS-derived structures were thermally and mechanically robust with their 3D structures well-maintained above 500 °C.[24] By treating the 3D POSS structures under Ar or O_2 plasma, we obtained crack-free samples over the entire patterned area (~5 mm in diameter).[26] Since the 3D POSS structures (both the original and oxidized ones) can be readily removed by HF etching at room temperature, these IL-patterned POSS-derived structures appeared to have the ideal properties needed for use as templates in the construction of high temperature nonoxide ceramic PCs with designed microstructures.

Allylhydridopolycarbosilane (AHPCS)[27,28] is a commercially available (Starfire) preceramic polymer that upon pyrolysis at 1100 °C converts in high yields to an oxygen-free amorphous SiC ceramic. AHPCS pyrolyses at higher temperatures produce crystalline β-SiC. AHPCS is a yellowish viscous liquid at room temperature and we found that it could be directly infiltrated into the 3D porous POSS template by capillary force (Figure 1a−c). A cross-sectional scanning electron microscopy (SEM) image is shown in Figure 1e of a diamond-like POSS template with face-centered cubic (fcc) translational symmetry that had been backfilled with AHPCS, then pyrolyzed at 1100 °C under Ar for 1 h. The template was nearly completely filled with the ceramic from the top to the bottom of the film. The small gap between the template and the infiltrated ceramic (see top-view SEM image in Figure 1e inset) most likely resulted from the large mismatch of the thermal coefficients

(10) Olivier, K.-H.; Ferro, G.; Dazord, J.; Marinova, M.; Lorenzzi, J.; Polychroniadis, E.; Chaudouët, P.; Chaussende, D.; Miele, P. *J. Cryst. Growth* **2009**, *311*, 2385.
(11) Sudarshan, T. S.; Maximenko, S. I. *Microelectron. Eng.* **2006**, *83*, 155.
(12) Spitsberg, I.; Steibel, J. *Int. J. Appl. Ceram. Technol.* **2004**, *1*, 291.
(13) Zhu, D.; Miller, R. A.; Nagaraj, B. A.; Bruce, R. W. *Surf. Coat. Technol.* **2001**, *138*, 1.
(14) Nicholls, J. R.; Lawson, K. J.; Johnstone, A.; Rickerby, D. S. *Surf. Coat. Technol.* **2002**, *151−152*, 383.
(15) Thornton, J.; Cookson, D.; Pescott, E. *Surf. Coat. Technol.* **1999**, *120−121*, 96.
(16) Vlasov, Y. A.; Bo, X. Z.; Sturm, J. C.; Norris, D. J. *Nature* **2001**, *414*, 289.
(17) Moon, J. H.; Ford, J.; Yang, S. *Polym. Adv. Tech.* **2006**, *17*, 83.
(18) Moon, J. H.; Yang, S. *Chem. Rev.* **2010**, *110*, 547.
(19) Campbell, M.; Sharp, D. N.; Harrison, M. T.; Denning, R. G.; Turberfield, A. J. *Nature* **2000**, *404*, 53.
(20) Moon, J. H.; Yang, S.; Dong, W. T.; Perry, J. W.; Adibi, A.; Yang, S. M. *Opt. Express* **2006**, *14*, 6297.
(21) Braun, P. V.; Zehner, R. W.; White, C. A.; Weldon, M. K.; Kloc, C.; Patel, S. S.; Wiltzius, P. *Adv. Mater.* **2001**, *13*, 721.
(22) Gratson, G. M.; Garcia-Santamaria, F.; Lousse, V.; Xu, M. J.; Fan, S. H.; Lewis, J. A.; Braun, P. V. *Adv. Mater.* **2006**, *18*, 461.
(23) Xu, Y.; Zhu, X.; Dan, Y.; Moon, J. H.; Chen, V. W.; Johnson, A. T.; Perry, J. W.; Yang, S. *Chem. Mater.* **2008**, *20*, 1816.
(24) Moon, J. H.; Seo, J. S.; Xu, Y.; Yang, S. *J. Mater. Chem.* **2009**, *19*, 4687.
(25) Liang, G. Q.; Zhu, X.; Xu, Y.; Li, J.; Yang, S. *Adv. Mater.* **2010**, DOI: 10.1002/adma.201001785.
(26) Xu, Y. A.; Zhu, X. L.; Yang, S. *ACS Nano* **2009**, *3*, 3251.
(27) Interrante, L. V.; Whitmarsh, C. W.; Sherwood, W.; Wu, H.-J.; Lewis, R.; Maciel, G. *Mater. Res. Soc. Symp. Proc.* **1994**, *346*, 593.
(28) Interrante, L. V.; Whitmarsh, C. W.; Sherwood, W. *Mater. Res. Soc. Symp. Proc.* **1995**, *365*, 139.

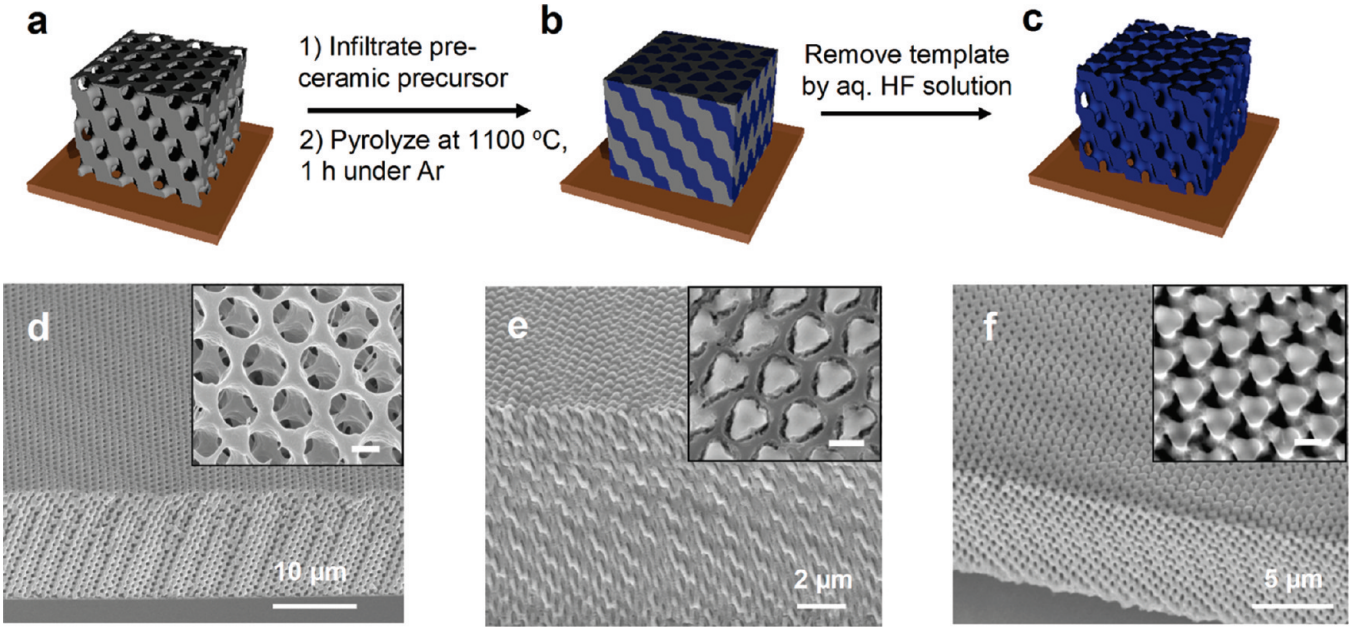

Figure 1. (a−c) Schematic illustration of the fabrication of a 3D ceramic structure from the 3D POSS template, (d−f) SEM images of 3D POSS template, (d) template/ceramic composite, (e) pyrolyzed at 1100 °C for 1 h under Ar, and (f) the inverse 3D ceramic structure after removal of the template. All the insets are the corresponding top views. Scale bars in insets: 500 nm.

of expansion at 1100 °C of the POSS template (or silica) and the infiltrated ceramic. After HF etching, an inverse 3D ceramic structure was obtained that closely replicated the POSS template (see Figure 1f). The 3-fold symmetry was clearly maintained in the (111) plane for an fcc lattice, while the triangular-like hole array in the POSS template was converted to an array of triangular-like ceramics. The lattice constant in the 3D ceramic structure became smaller due to film shrinkage at the high temperature; however, the number of layers remained the same, ~12. Quantitative comparisons of the periodicity of the 3D ceramic structures at different thermal treatment conditions will be discussed later.

To confirm the ceramic composition within the 3D template and investigate the chemical nature of the resulting ceramics at the different pyrolysis temperatures, the elemental compositions of the materials were measured by energy-dispersive X-ray (EDX) mapping analysis along with their FT-IR spectra. Measurements from bulk ceramic films treated under the same conditions were used as reference.

As can be seen in Table 1, the EDX data indicated that there was excess carbon and appreciable oxygen contained in both the 3D and bulk ceramic films generated at 1100 °C with ~1:0.96:3.46 Si:O:C ratios in the 3D ceramic film and ~1:0.23:1.29 ratios in the bulk film. The excess carbon is consistent with the SiC/C ceramic compositions that have been obtained from the AHPCS precursor.[29] Since the AHPCS ceramic precursor does not contain oxygen, the observed oxygen contents must either come from reactions of the films with the POSS template or by reactions with trace O_2 in the Ar during pyrolysis. The larger oxygen content of the 3D film compared to the bulk film, is most likely a result of the surface passivation of the much larger surface area of the porous 3D structure. It has been suggested that the oxygen that is often incorporated in the silicon carbide ceramics prepared from the polycarbosilane precursor is present as SiO_2 on the ceramic surface.[30] The EDX measurements suggest the possibility of silicon oxycarbide formation, since the observed elemental ratios are in the ranges for such ceramics. Silicon oxycarbides have typically been prepared by pyrolysis between 800 and 1400 °C of silicon-containing polymers or sol-gel precursors of organosilicates.[31−33] They contain both Si-C and Si-O bonds with the general formula SiO_xC_y where $x < 2$ and can be viewed as mixtures of $SiO_{4/2}$, $SiO_{3/2}C_{1/4}$, $SiO_{2/2}C_{2/4}$, $SiO_{1/2}C_{3/4}$, $SiC_{4/4}$,[33] with the relative amounts determined by the O/Si ratio. Depending on the C and O concentrations, they can be further classified as being like SiC, Si-O-C or SiO_2 materials,[33,34] with each class having very different mass densities and refractive index properties. For example, SiC-like materials have the highest refractive index, 2.4−3.1, whereas Si-O-C and SiO_2-like materials have refractive indices of 1.76−1.85 and 1.5, respectively.[34] The high refractive index of ~2.65 that was measured, as discussed later, for the 3D material formed at 1100 °C indicates that it is a SiC-like material.

(29) Mutin, P. H. *J. Sol-Gel Sci. Technol.* **1999**, *14*, 27.
(30) Yajima, S.; Okamura, K.; Matsuzawa, T.; Hasegawa, Y.; Shishido, T. *Nature* **1979**, *279*, 706.
(31) Chi, F. K. *Ceram. Eng. Sci. Proc.* **1983**, *4*, 704.
(32) Renlund, G. M.; Prochazka, S.; Doremus, R. H. *J. Mater. Res.* **1991**, *6*, 2716.
(33) Zank, G. A., Preceramic Polymer-derived Silicon Oxycarbides. In *Silicon-Containing Polymers-The Science and Technology of Their Synthesis and Applications*; Jones, R. G.; Ando, W.; Chojnowski, J., Eds.; Kluwer Academic Publishers: Norwell, MA, 2000; pp 697.
(34) Gallis, S.; Nikas, V.; Suhag, H.; Huang, M.; Kaloyeros, A. E. In A Comparative Study of a-SiCxOyHz Thin Films Grown via Chemical Vapor Deposition for Silicon Photonics, Nanoengineering: Fabrication, Properties, Optics, and Devices V 2008; Dobisz, E. A.; Eldada, L. A., Eds.; Proceedings of SPIE, **2008**; p 70390L.

Table 1. Elemental C, O and Si Contents by EDX in the Ceramic Films (Both 3D and Bulk) Pyrolyzed at 1100 or 1300 °C for 1 h under Ar or Vacuum Environments[a]

Materials	C	O	Si
Inverse 3D ceramic, 1100 °C under Ar	63.59	17.63	18.36
Bulk ceramic film, 1100 °C under Ar	51.17	9.17	39.65
Inverse 3D ceramic after additional sintering at 1300 °C in vacuo*	51.04	0.60	44.24
Bulk ceramic film, 1300 °C in vacuo	53.66	0	46.34

[a] All films were supported on Si wafers. *Trace contaminants: Fe 3.37% and Ni 0.75%.

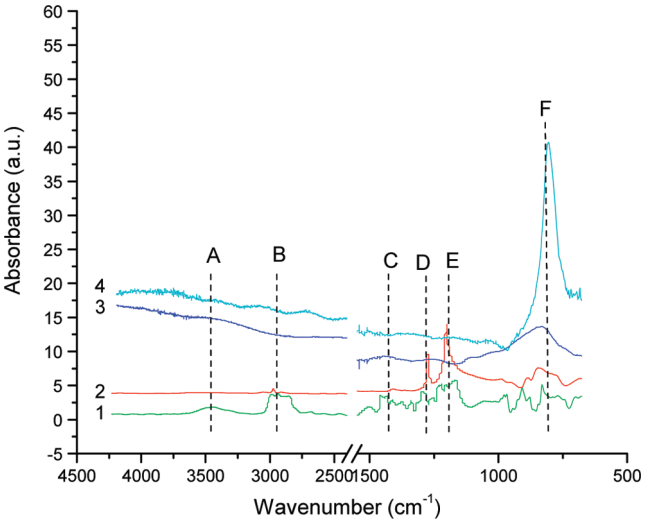

Figure 2. FTIR spectra of bulk POSS and inverse 3D ceramic films treated under different conditions. (1) Bulk POSS film. (2) Bulk POSS film pyrolyzed at 1100 °C for 1 h under Ar. (3) Inverse 3D ceramic film pyrolyzed at 1100 °C for 1 h under Ar. (4) Inverse 3D ceramic film pyrolyzed for additional 1 h at 1300 °C in vacuo. Peak A: OH stretch; B: CH_2 stretch; C: CH_2 deformation; D: CH_3 deformation; E: O-Si-O vibration; F: Si-C stretch.

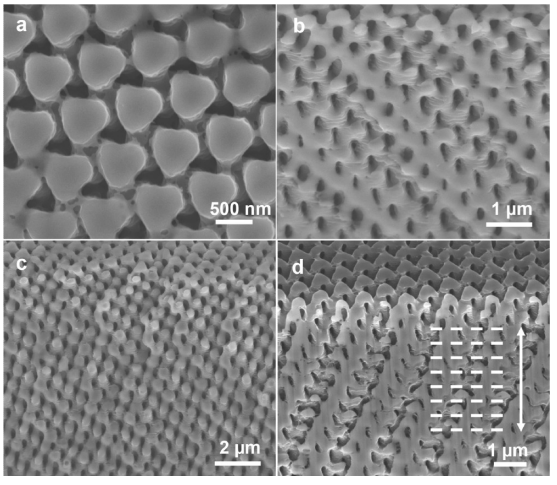

Figure 3. SEM images of the inverse 3D ceramic film of Figure 1 following additional pyrolysis at 1100 °C for 1 h in vacuo. (a) Top view, (b, c) Cross-sectional views in different plane directions, (d) Cross-sectional view of the sample FIB milled perpendicularly to the (111) plane with an output current of 1000 pA, and sample tilt at 52°.

This conclusion is supported by the FT-IR spectrum (Figure 2) of the 3D ceramic film, which showed a much stronger Si-C stretching (peak F, 812 cm^{-1}) relative to the O-Si-O vibration (peak E, 1063 cm^{-1}). Likewise, the fact that the 3D ceramic film, unlike the SiO_2 template, did not dissolve in aqueous HF solution indicates

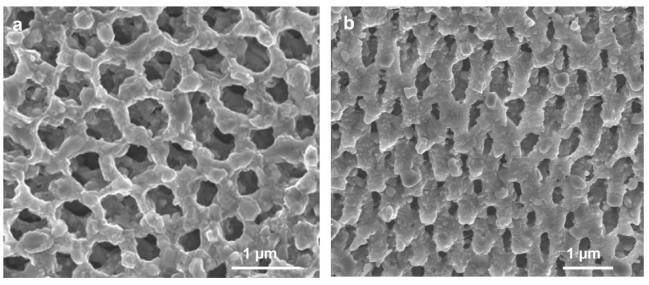

Figure 4. SEM images of inverse 3D ceramic film following additional pyrolysis at 1300 °C in vacuo (5×10^{-5} mTorr) for 1 h, showing the onset of β-SiC crystallization. (a) Top view. (b) Cross-sectional view.

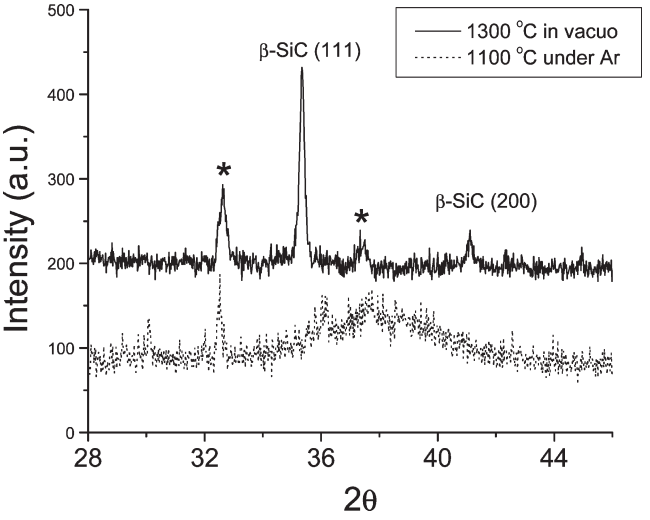

Figure 5. X-ray diffraction (XRD) spectra of bulk ceramic films pyrolyzed at different temperatures. *: peaks from Si substrate.

that it has properties more consistent with a SiC-like ceramic.[35,36]

Silicon oxycarbides are known to undergo carbothermic reduction at higher temperatures (≥1300 °C) to produce SiC with loss of carbon monoxide[37−39] and crystallization to β-SiC Carbothermal reduction of higher carbon content silicon oxycarbide yields silicon carbide with residual C.[39] Consistent with the literature, an oxygen-free 3D film with a near stoichiometric $Si_{1.0}C_{1.15}$ ratio was achieved when the 1100 °C generated inverse 3D ceramic film was pyrolyzed at 1300 °C for 1 h in vacuo (see Table 1

(35) Guan, G.; Kusakabe, K.; Ozono, H.; Taneda, M.; Uehara, M.; Maeda, H. *Chem. Eng. J.* **2008**, *135*, 232.
(36) Pena-Alonso, R.; Mariotto, G.; Gervais, C.; Babonneau, F.; Soraru, G. D. *Chem. Mater.* **2007**, *19*, 5694.
(37) White, D. A.; Oleff, S. M.; Boyer, R. D.; Budinger, P. A.; Fox, J. R. *Adv. Ceram. Mater.* **1987**, *2*, 45.
(38) White, D. A.; Oleff, S. M.; Fox, J. R. *Adv. Ceram. Mater.* **1987**, *2*, 53.
(39) Saha, A.; Raj, R. *J. Am. Ceram. Soc.* **2007**, *90*, 578.

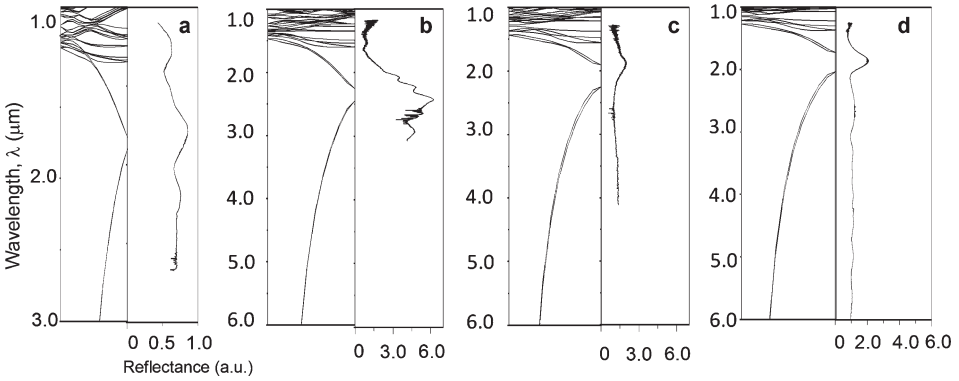

Figure 6. FT-IR reflectance spectra of 3D diamond-like structures in the [111] direction. (a) Unfilled 3D POSS template. (b) 3D template/ceramic composite pyrolyzed at 1100 °C for 1 h under Ar. (c) Inverse 3D ceramic (silicon oxycarbide) after template removal. (d) Inverse 3D silicon carbide obtained after additional heating of the silicon oxycarbide film to 1300 °C for 1 h in vacuo. In each panel, the left figure is a simulated spectrum and the right one is the experimental FT-IR spectrum.

Table 2. Comparisons of the Lattice Constants of 3D POSS Template and Ceramic Structures Obtained at Different Stages

	3D unfilled POSS template	3D ceramic/POSS composite pyrolyzed at 1100 °C under Ar	Inverse 3D ceramic film pyrolyzed at 1100 °C under Ar	Inverse 3D ceramic film with additional in vacuo sintering at 1100 °C	Inverse 3D ceramic film with additional in vacuo sintering at 1300 °C
Pitch in the (111) plane (μm)	0.98	0.79	0.79	0.76	0.72
Distance between the adjacent planes in the [111] direction (μm)	0.68	0.59	0.59	0.57	0.55

and Figure 2). While the SEM images of the 3D films generated at 1100 °C appeared amorphous (Figure 3), the 3D films prepared at 1300 °C in vacuo appeared crystalline with crystallite sizes of ~10 nm (Figure 4). The sharp peaks at 35.4° and 41.1° 2θ in the X-ray diffraction (XRD) data of the 1300 °C bulk ceramic film indicate, as normally found for AHPCS-derived ceramics, β-SiC crystallization (see Figure 5).[40,41]

As can be seen by comparing Figures 3 and 4, the onset of crystallization leads to some distortion in the 1300 °C PC array. Further annealing at higher temperature would increase the degree of crystallization and the resulting grain growth would degrade the uniformity of the array. Thus, to maintain the structural integrity of these materials at higher temperatures, it will be necessary to retard ceramic crystallization by, for example, the addition of other elements such as boron.[42,43]

The lattice constants of the 3D structures measured at different processing stages are summarized in Table 2. The lattice parameter in the (111) plane was measured from the top-view SEM images by averaging over two samples at three different locations.[44] At each location, we drew lines in three different directions. The distance between the adjacent lattice planes in the [111] direction was measured from the focus-ion-beam (FIB) milled cross-section with the FIB normal to the sample surface. Compared to the 3D POSS structure, the ceramic/POSS composite (Figure 1e) had ~13.2% shrinkage in the vertical direction and 19.4% shrinkage in the (111) plane after being pyrolyzed at 1100 °C under Ar. The relatively large shrinkage in the (111) plane and the thermal coefficient of expansion mismatch between the film and the substrate (Si) led to many microcracks in the pyrolyzed samples. However, locally crack-free single domains over at least 100 μm by 100 μm areas could be readily found, allowing for SEM and FT-IR characterizations. There was almost no change in the lattice constants of the inverse 3D silicon oxycarbide structures after removal of the POSS template by aq. HF etching (see Table 2).

The inverse 3D ceramic photonic crystals were stable up to 1300 °C under an inert atmosphere. As seen in Figure 3, the 3D structure was well-maintained with only a small dimensional change after the additional pyrolysis in vacuo, with only 3.8% and 8.9% shrinkages in the (111) plane at 1100 and 1300 °C, respectively, and 3.4% and 6.8% in the [111] direction, respectively (see Table 2).

To evaluate the photonic bandgap properties of these newly synthesized 3D ceramic photonic crystals, FT-IR was used to measure the reflectance of the 3D structures, including the unfilled POSS template, ceramic/template composite, and the inverse ceramic films obtained at different processing conditions. The results were then compared with the calculated PBGs. As can be seen in Figure 6a, a stop band peak at 1.78 μm was observed from the unfilled 3D POSS template. For the ceramic filled composite pyrolyzed at 1100 °C under Ar, there was a bathochromic shift of the reflection peak to ~2.45 μm (Figure 6b). This shift is expected due to the increase in the mean refractive index of the ceramic/template composite structure. After removal of the template, a blue shift of the stop band to 1.84 μm was observed for the inverse 3D ceramic structure (Figure 6c) since the mean refractive index was

(40) Krishna, P.; Marshall, R. C. *J. Cryst. Growth* **1971**, *11*, 147.
(41) Krishna, P.; Marshall, R. C. *J. Cryst. Growth* **1971**, *9*, 319.
(42) Boakye, E. E.; Mogilevsky, P.; Parthasarathy, T. A.; Hay, R. S.; Welter, J.; Kerans, R. J. *J. Am. Ceram. Soc.* **2006**, *89*, 3475.
(43) Kerans, R. J.; Hay, R. S.; Parthasarathy, T. A.; Cinibulk, M. K. *J. Am. Ceram. Soc.* **2002**, *85*, 2599.
(44) Zhu, X.; Xu, Y.; Yang, S. *Opt. Express* **2007**, *15*, 16546.

decreased. The peak reflectivity increased significantly from 0.8 (3D unfilled POSS) to 2.0 (inverse 3D ceramic), indicating an increased optical quality of the films. Additionally, we observed that the ceramic/template composite film was the most colorful with the highest reflectivity of 6.2. This result is different from our previous observation from titania infiltrated polymer templates.[23] This difference may be due in part to the small air gap between the infiltrated ceramic and the template structure (Figure 1e) and the larger mean refractive index for the composite compared to that of the inverse 3D structure. The experimental reflectivity peak positions at different processing stages agree well with the calculated bandgaps, further supporting the high quality of the backfilling and the resulting 3D ceramic photonic crystals. In the calculations, 1.52,[26] 1.45[45] and 2.65 were used as the reflective indices of the POSS at room temperature, the POSS after heating to 1100 °C (converted to silica-like materials), and the SiC-like silicon oxycarbide obtained at 1100 °C under Ar, respectively. In the composite film, we considered ~5% air and 52.5% filling volume fraction of the ceramic based on SEM images. Since the refractive index of the 3D ceramic film cannot be directly measured, the experimentally observed bandgap was fitted with the theoretical simulation to calculate its refractive index. The high value of 2.65 suggests that the ceramic film pyrolyzed at 1100 °C under Ar is indeed SiC-like.[34] When the 3D ceramic film was further heated at 1300 °C in vacuo, the resulting 3D SiC material had a refractive index of 2.56 that is close to both the literature value[45] of 2.55 for all SiC polytypes and that experimentally measured for the ceramic PC obtained at 1100 °C under Ar. After additional heating to 1300 °C in vacuo, the absolute reflectance was slightly increased to 2.10, but because of the small changes in the refractive index and volume filling fractions, 52.5% to 45%, the stop band position remained at 1.84 μm (Figure 6d). The high reflectivity of the photonic band gaps observed in the ceramic films and their match with simulation clearly provide evidence of the high quality of the ceramic photonic crystals synthesized through the IL-patterned POSS templates. Even with the distortion arising from the onset of SiC crystallization at 1300 °C, the PC structure and bandgap position were well maintained.

Conclusions

The fabrication of diamond-like 3D silicon-oxycarbide and silicon-carbide ceramic photonic crystals have been achieved by using four-beam interference lithography (IL) in conjunction with templating via a polymeric precursor backfilled into 3D POSS structures. FT-IR and EDX analysis suggested that the 3D ceramic films pyrolyzed at 1100 °C under Ar are SiC-like silicon oxycarbide. Further thermal treatment at 1300 °C in vacuo converted the amorphous ceramic film to oxygen-free crystalline 3D β-SiC. The 3D ceramic structures were highly thermally stable: additional pyrolysis above 1100 °C in vacuo showed only 2.5% and 8.9% shrinkages in the (111) plane at 1100 and 1300 °C, respectively, and 3.4% and 6.8% in the [111] direction, respectively. A comparison of the calculated photonic bandgap properties to the measurements of film reflectivity in the [111] direction before and after the ceramic conversion suggested that the template was nearly completely filled by the ceramic, with the photonic structure being preserved after the removal of the template. Although template syntheses of high-temperature ceramics have previously been achieved using nanofiber, nanotube, colloidal-particle, block-copolymer, and 3D diatom[46−53] templates, the laser-based IL technique offers an efficient and versatile route to create a wide range of photonic structures by careful design of appropriate optical setups. This templating approach using 3D organosilicate structures in conjunction with an appropriate preceramic precursor should now allow the fabrication of a variety of highly robust 3D nonoxide ceramic photonic crystals. As will be reported elsewhere, we have in fact already used this method to fabricate 3D boron carbide structures from the 3D POSS structure by backfilling with the bis(decaboranyl)hexane ceramic precursor.[54]

Experimental Methods

Fabrication of 3D POSS Structures. The 3D POSS structure was fabricated by four-beam interference lithography using the same optical setup reported earlier.[23] Briefly, the central beam of a visible diode-pumped Nd:YVO_4 laser (Coherent, Verdi V6, λ = 532 nm) was circularly polarized with normal incidence to the photoresist film, while the other three surrounding beams were linearly polarized and oblique at 39° relative to the central one. The wave vectors of four beams were $\boldsymbol{k}_0 = \pi/a[333]$, $\boldsymbol{k}_1 = \pi/a[511]$, $\boldsymbol{k}_2 = \pi/a[151]$, and $\boldsymbol{k}_3 = \pi/a[115]$, respectively. The polarization vectors of beam 1, 2, and 3 were $e_1 = [-0.250, 0.345, 0.905]$, $e_2 = [0.905, -0.250, 0.345]$, and $e_3 = [0.345, 0.905, -0.250]$, respectively. The circular polarization of the central beam distributed the intensity equally to the surrounding beams, at a ratio of 1.8:1:1:1.

The photoresist solution (~80 wt %) was formulated by mixing epoxycyclohexyl POSS cage mixture (EP0408, Hybrid Plastics) and 1.0 wt % Irgacure 261 (Ciba Specialty Chemicals) as visible photoinitiators in propylene glycol monomethyl ether acetate (PGMEA, Aldrich). After spin coating the photoresist solution on an oxygen plasma (PDC-001, Harrick Scientific Products, Inc.) cleaned silicon wafer at 2000 rpm for 30 s, followed by prebaking at 50 °C for ~40 min and 95 °C for 2 min, a ~8 μm thick POSS film was obtained. After exposure to four-interfering beams (power of beam source ~0.7 w) for ~1 s, the film was postexposure baked at 50 °C for 30 s and then developed in PGMEA to obtain the 3D microporous structures. The films were dried

(45) Lide, D. R., *CRC Handbook of Chemistry and Physics*, 82nd ed.; CRC Press: Boca Raton, FL, 2001−2002.
(46) Pender, M. J.; Sneddon, L. G. *Chem. Mater.* **2000**, *12*, 280.
(47) Sneddon, L. G.; Pender, M. J.; Forsthoefel, K. M.; Kusari, U.; Wei, X. L. *J. European Ceram. Soc.* **2005**, *25*, 91.
(48) Kusari, U.; Bao, Z.; Cai, Y.; Ahmad, G.; Sandhage, K. H.; Sneddon, L. G. *Chem. Commun.* **2007**, 1177.
(49) Jones, B. H.; Lodge, T. P. *J. Am. Chem. Soc.* **2009**, *131*, 1676.
(50) Pashchanka, M.; Engstler, J.; Schneider, J. J.; Siozios, V.; Fasel, C.; Hauser, R.; Kinski, I.; Riedel, R.; Lauterbach, S.; Kleebe, H. J.; Flege, S.; Ensinger, W. *Eur. J. Inorg. Chem.* **2009**, *23*, 3496.
(51) Takagi, K.; Takahashi, T.; Kikuchi, K.; Kawasaki, A. *J. Eur. Ceram. Soc.* **2010**, *30*, 2049.
(52) Niu, L. F.; Kua, H. Y.; Chua, D. H. C. *Langmuir* **2010**, *26*, 4069.
(53) Xiao, Z. Y.; Wang, A. J.; Kim, D. P. *J. Mater. Chem.* **2010**, *20*, 2853.
(54) Pender, M. J.; Carroll, P. J.; Sneddon, L. G. *J. Am. Chem. Soc.* **2001**, *123*, 12222.

Scheme 1. Chemical Structures of the Template Material, Epoxycyclohexyl POSS, and the Ceramic Precursor, AHPCS

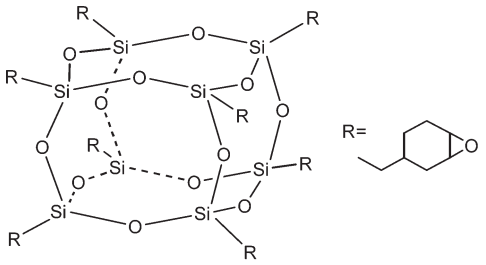

Epoxycyclohexyl POSS

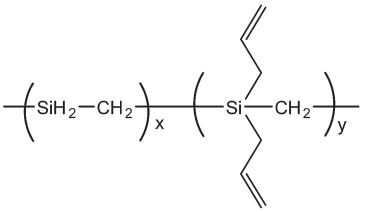

Allylhydridopolycarbosilane (AHPCS)

in a supercritical CO_2 dryer (SAMDRI-PVT-3D, tousimis) to prevent pattern collapse.

Template Fabrication of the 3D Ceramic Photonic Crystals. To obtain the 3D ceramic photonic crystals, the AHPCS liquid precursor (allylhydridopolycarbosilane from Starfire Systems, used as received except that any volatile impurities were initially removed by pumping under high vacuum) was infiltrated into the 3D POSS template through capillary action. To minimize the formation of any overcoat on top of the template, a droplet of AHPCS liquid was placed at the side of the 3D POSS film and kept in contact for ~30 min to achieve complete filling. The infiltrated AHPCS was then converted to the ceramic at 1100 °C under Ar for 1 h at a heating rate of 10 °C/min in a thermal gravimetric analysis (TGA) sample pan (TA Instruments, SDT 2960 simultaneous DTA-TGA). After cooling to room temperature, the sample was immersed in an aqueous HF solution (~20 wt %) for ~4 h to remove the POSS template, and then rinsed with DI water at least five times before characterization.[26] As a reference, the bulk ceramic film (thickness $>8\ \mu$m) was prepared by spin coating AHPCS onto a silicon wafer, followed by pyrolysis under the same conditions as that used for the 3D ceramic PCs (Scheme 1).

The above obtained ceramic films (both 3D and bulk) were further heated to 1100 and 1300 °C, respectively, in vacuo ($\sim 1 \times 10^{-5}$ mTorr) in a tube furnace at a rate of 10 °C/min, and held for 1 h to investigate their thermal stability.

Characterization. High resolution SEM images were taken from the FEI Strata DB235 Focused Ion Beam (FIB) system at 5 kV. The lattice constant in the (111) plane was measured from the top-view SEM images by averaging over two samples at three different locations, each having data points drawn from three different directions. The distance between the adjacent lattice planes in the [111] direction was measured from the FIB milled cross-section. The samples were cut by FIB normal to the surface at an acceleration current of 1000 pA. The film shrinkage was estimated by comparing the measured lattice constants to the theoretically calculated values.[44] The FT-IR spectra were acquired on a Nicolet 8700 equipped with Nicolet continuum infrared microscope. The samples were measured in the reflection mode with a MCT detector in the [111] direction, and an aperture size of $\sim 80 \times 80\ \mu$m. The photonic bandgap properties of the crystal structures obtained at the different processing steps were calculated with the MIT Photonic-Band Package, where the refractive indices of 1.52,[26] 1.45,[45] 2.65, and 2.56[45] were used for POSS, silica, SiC-like silicon oxycarbide, and silicon carbide, respectively. The overall chemical compositions and distribution of the chemical elements in the 3D structures were determined by energy-dispersive X-ray (EDX) analysis on a high resolution field emission scanning electron microscope (FESEM) JEOL 7500F coupled to an Oxford Si/Li detector and INCA software. The EDX spectra were collected at an acceleration voltage of 13 KeV. Since the 3D SiC films were thick ($\sim 8\ \mu$m), the samples were supported on a silicon wafer for EDX measurement after confirming the same element compositions on a tantalum substrate.

Acknowledgment. This research was supported by Air Force of Scientific Research (AFOSR), Grant No. FA9550-06-1-0228, and in part by the Office of Naval Research (ONR), Grant No. N00014-05-0303. We are grateful to Dr. Charles Lee (AFOSR) for motivating this research. We thank Dr. Angang Dong and Prof. Chris Murray for access to the FT-IR. We acknowledge the Penn Regional Nanotechnology Facility (PRNF) for access to SEM and EDX analysis. We also thank Mr. Steve Szewczyk for setting up the furnace for heat treatment under vacuum conditions.